A satellite-derived re-analysis of surface-ocean pH variability in the coastal waters of India

Vinaya Kumar Vase*, Rajan Kumar, Shikha Rahangdale, Sanjana Kartu, Harshad Solanki, Jayasankar Jayaraman, Ratheesh Kumar and Grinson George
Indian Council of Agricultural Research-Central Marine Fisheries Research Institute, Kochi 682 018, India

Monitoring pH variations in coastal waters is essential for maintaining marine life and developing strategies to combat ocean acidification caused by climate change. The present study examines pH changes on interannual and seasonal scales along the northwest (NW), southwest (SW), southeast (SE), and northeast (NE) coasts of India over 30 years (1993–2022) using satellite data. Results reveal a significant decline in pH levels ($R^2 = 0.727$) across Indian coastal waters, with notable regional differences. The northeastern coast showed the greatest pH stability and the smallest decrease ($R^2 = 0.798$), while the southwestern coast experienced the highest variability ($R^2 = 0.490$). These regional pH fluctuations suggest varying resilience to ocean acidification. The NE and SW coasts, with higher variability, may be more susceptible to environmental changes, underscoring the importance of targeted monitoring and mitigation measures. In contrast, the more stable trends along the SE and NW coasts present opportunities to explore long-term resilience mechanisms. Seasonal fluctuations were evident everywhere, with winter consistently showing higher pH values and monsoon seasons the lowest. Principal component analysis indicated that the first two components accounted for 85.7% of the variance, highlighting factors such as seasonal river inflows, biological activity, and monsoonal freshwater input. Overall, these findings emphasise the importance of region-specific coastal management strategies to address climate change impacts and human pressures, while also providing a baseline for tracking future ocean acidification trends and assessing their effects on marine biodiversity and ecosystem services.

Keywords: Acidification, coastal waters, Indian EEZ, satellite-derived data, spatial variability.

OCEAN acidification is a major global concern linked to climate change, as the ocean has absorbed over 30% of human-made CO_2 emissions from the atmosphere. Globally, research focuses on understanding how declining pH levels affect calcifying organisms, such as corals, molluscs, bottom-living biota, and plankton, which are essential to marine food webs[1]. The large uptake of CO_2 by the oceans decreases pH (measured as the negative logarithm of H^+ ion concentrations), resulting in the formation of carbonic acid that harms marine life[2]. The changes in water pH caused by biochemical and biogeochemical reactions mainly affect calcifying organisms due to the lower saturation of $CaCO_3$ in seawater[3]. The rate of acidification is higher in coastal areas than offshore regions due to nearby anthropogenic activities and land influence that alter carbonate chemistry[4].

The oceans are predicted to become more acidic due to the exceeding atmospheric concentrations of CO_2 at 415 ppmv, and this trend is expected to continue, surpassing the pre-industrial level of 280 ppmv (ref. 2). Several studies have projected a decline of upper ocean pH by 0.3–0.4 units by the end of the 21st century[5], which can reduce oceanic biological production[6]. Modelling experiments conducted by Caldeira and Wickett[7] and Orr[8] suggest a decrease in surface ocean pH of about 0.3 from current conditions by the end of this century, based on estimates of future CO_2 emissions. Spatial and seasonal dynamics in pH at the global scale and their potential impact on biogeochemical cycles and marine biota were studied[3,9–12]. Researchers employ a combination of satellite datasets, numerical models, and *in situ* observations to assess spatiotemporal trends in pH and its drivers, including anthropogenic CO_2 emissions and natural variability[13].

Although a few coastal pH measurements exist, the observations to study acidification in the Indian Ocean are unavailable at a basin scale to depict a comprehensive understanding of acidification[14]. The pH measurements were made sporadically at short periods and limited locations along the coastal waters of western India[15–18] and eastern India[19–21], which fails to bring a synoptic view of the variability of pH at spatial and temporal scales. Time-series monitoring of pH through field survey techniques is costly and time-consuming, especially for wider-area and long-term investigations[22]. To overcome these limitations, we use a satellite-derived pH reanalysis to examine spatial and temporal variability in coastal Indian waters to understand the signs of ocean acidification. The present study aimed to address two research objectives: i) inter-annual variability in satellite-derived pH variability along the Indian coast and ii) spatial and seasonal dynamics in pH

*For correspondence. (e-mail: v.vinaykumarvs@gmail.com)

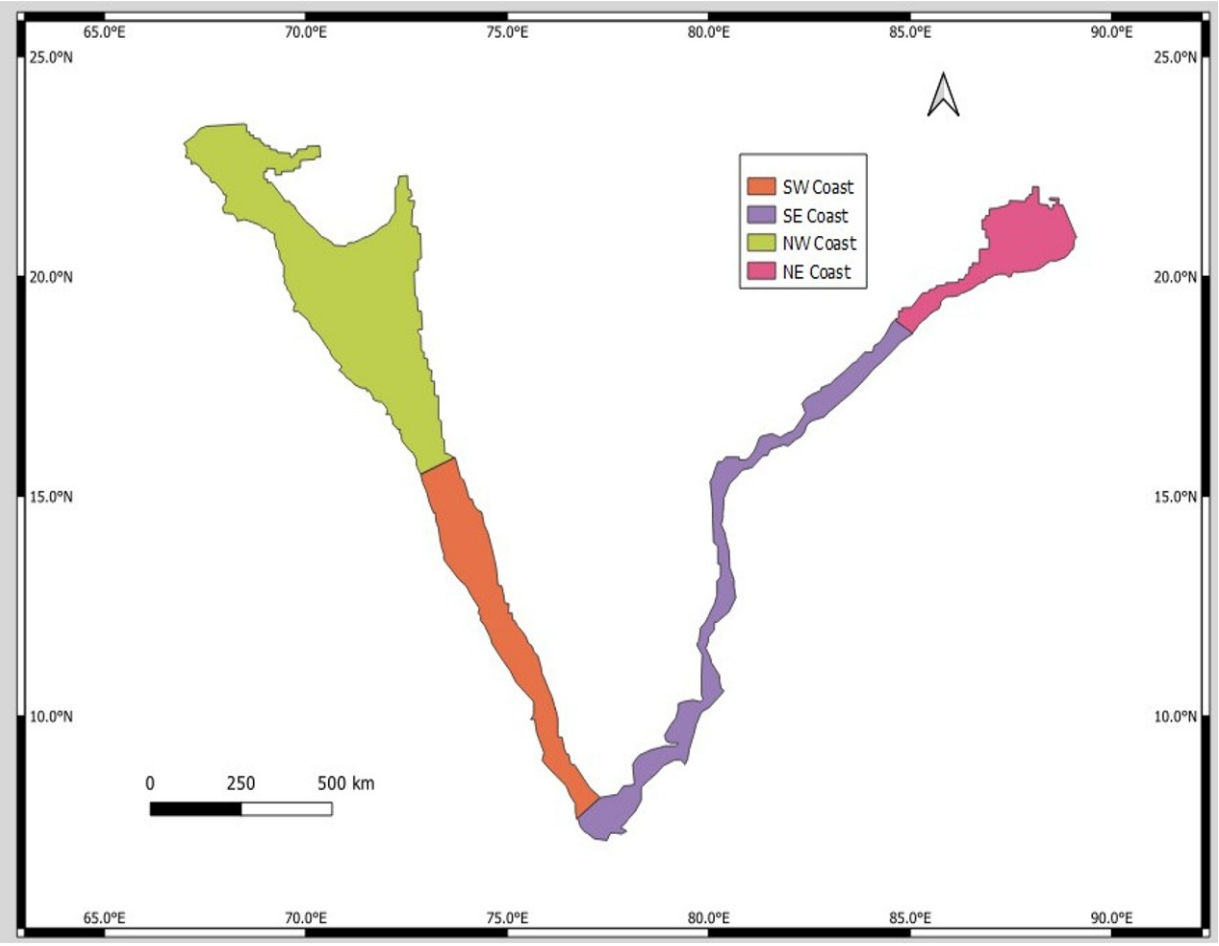

Figure 1. Area of interest to analyse spatial and temporal variability. SW, Southwest; SE, Southeast; NW, Northwest; NE, Northeast.

across the Indian coastal waters using multivariate analysis. These efforts are critical for developing climate adaptation and conservation strategies in Indian waters. The spatio-temporal variability in pH will help to frame an adaptive strategy to mitigate the effects of ocean acidification on marine biodiversity and fishery resources.

Methodology

Study area and period

The coastal waters of India up to 200 m depth were identified as an area of interest (AOI) (Figure 1). The satellite-derived pH data were spatially segregated into four distinct coastal regions: northwest (NW), southwest (SW), southeast (SE), and northeast (NE). The satellite-derived seawater pH reported on the total scale was retrieved from Copernicus Marine Service for 30 years (1993–2022) (ref. 23, 24). To investigate temporal variability in pH, the data were delineated into four seasons: winter, pH_W (December to February), summer, pH_S (March to May), monsoon, pH_M (June to September), and post-monsoon, pH_PM (October to November). This classification ensures a comprehensive understanding of regional and seasonal variability in pH levels along the Indian coastline.

Satellite-derived pH data

The higher temporal frequency and extensive spatial coverage of pH data could be successfully obtained using remote sensing techniques. The Copernicus Marine Service dataset, a robust repository of oceanographic data, offers high-resolution spatial and temporal data on pH levels. The pH level-4 product (Copernicus Marine Environment Monitoring Service, GLOBAL_MULTIYEAR_BGC_001_029, Biogeochemical Re-Analysis v5.2) was processed with $0.25° \times 0.25°$ spatial and monthly temporal resolutions, and 75 vertical levels were employed to investigate pH variability in the coastal waters of India[25]. The pH product was evaluated using 62 coastal profiles from GO-SHIP and 48

Biogeochemical Argo (BGC-Argo) floats (2005–2021) and depicts robust validation statistics of mean bias (–0.014), root mean square error (0.046), and correlation ($r = 0.83$) ($p < 0.001$) (ref. 26). The product was downloaded in NetCDF-4 format and processed through the SeaDAS 7.5.1 version software[27]. The number of pixels varied for different zones (NW, SW, SE, and NE) and the spatial range (geocoordinates) (Table 1).

Data processing and analysis

Data preprocessing is carried out using SeaDAS (Seaviewing Wide Field-of-view Sensor Data Analysis System), a specialised software for ocean-colour data[27]. The software is employed to process raw satellite imagery, correcting for atmospheric interference, radiometric errors, and other distortions to ensure accurate pH retrieval. Region-specific spatial shapefiles are created in SeaDAS to extract pH data corresponding to each coast. The pH values for different coasts were retrieved by importing shape files of coasts and extracting them using the mask pixel import technique. Spatial analysis and visualisation exercises are conducted using Quantum Geographic Information System (QGIS), an open-source geographic information system[28]. pH variability maps are generated for each coast and season, revealing spatial and temporal patterns. The combined use of SeaDAS for preprocessing pH data and QGIS for spatial analysis ensures a robust methodological framework for understanding coastal pH dynamics. Analysis of variance and principal component analysis (PCA) analysis were performed using R 4.4.0 software.

Results

The annual trend of pH values from 1993 to 2022 shows a general decline trend, with occasional minor fluctuations (Figure 2). Starting in 1993, the pH value was around 8.08, and it gradually increased slightly over the following years, peaking at 8.09 in 1995. However, from the late 1990s onwards, the trend shows a slight decrease, with pH values dipping to around 8.06 by 2009. The decrease continued through the 2010s, reaching a low of 8.05 in 2016 and 2017. In 2018, a brief uptick occurred, bringing the pH back to approximately 8.05, before a stable range of 8.05 to 8.07 persisted in the final years, 2020–2022. A significant decrease in pH was observed along the four coasts, and higher values were observed along the north-east ($R^2 = 0.798$), followed by south-east ($R^2 = 0.716$), north-west ($R^2 = 0.714$), and south-west ($R^2 = 0.490$) (Table 2). In terms of inter-annual variation, pH levels for the NW, SW, and SE regions generally show little change, with values hovering around 8.06 to 8.08, while the NE region shows more variation, with pH levels ranging from 8.08 to 8.14. Over the years, the pH levels in the NW and SW regions have gradually declined, though the overall decline is minimal. The SE region shows a slight downward trend, but values remain above 8.0. On the other hand, the NE region remains slightly more alkaline than the other regions, consistently staying above 8.0 and experiencing very little fluctuation.

Coast-wise pH variability

The pH along the northwest coast exhibited clear seasonal variations. The lowest pH values were recorded during the monsoon (8.053 ± 0.017), while winter showed the highest pH levels (8.085 ± 0.022), and summer displayed relatively stable values (8.062 ± 0.006). One-way analysis of variance (ANOVA) confirmed a significant seasonal effect on pH ($F(3, 356) = 76.11$, $p < 0.0001$). The Tukey post hoc analysis revealed highly significant differences between winter and monsoon and winter and post-monsoon (both $p < 0.0001$), and summer and monsoon ($p = 0.0183$), while no significant difference was observed between post-monsoon and summer ($p = 0.9984$) (Table 3). Spatially, a north-to-south gradient was evident, with northern regions exhibiting higher pH values (Figure 3 *a*). These results highlight minor but significant seasonal and spatial pH fluctuations, with the highest pH during winter and the lowest during the monsoon. A slight seasonal variation was observed in pH along the southwest coast, but it remained consistently alkaline with minimal fluctuations. Winter recorded the highest mean pH (8.061 ± 0.008), but a lower pH was observed during the post-monsoon season (8.021 ± 0.013). A highly significant seasonal effect on pH was observed ($F(3, 356) = 66.5$, $p < 0.0001$), with Tukey post hoc tests identifying substantial differences between winter and all other seasons ($p < 0.0001$) (Table 3). No significant difference was found between summer and monsoon ($p = 0.7827$). Spatially, northern regions show slightly higher pH values than the southern regions across all seasons along the south-west coast (Figure 3 *b*).

Notable seasonal variations were observed in pH values along the southeast coast of India, with the lowest values during the monsoon (8.029 ± 0.013) and the highest during winter (8.100 ± 0.018). Post-monsoon pH increased slightly (8.070 ± 0.030), while summer values remained relatively stable (8.046 ± 0.008). One-way ANOVA revealed a highly significant seasonal variation in pH ($F(3, 356) = 297.2$, $p < 0.0001$), with Tukey post hoc tests identifying significant differences across all seasonal comparisons ($p < 0.0001$) (Table 3). These results indicate minor but significant seasonal fluctuations, with winter pH consistently higher than other seasons. Spatially, the pH distribution along the southeast coast shows a clear gradient, with northern regions exhibiting higher values than the southern parts across all seasons (Figure 3 *c*). The pH along the northeast coast of India indicated clear seasonal

Table 1. Spatial details of coastal regions in India, including latitude, longitude, resolution and number of pixels

Type of coast	Latitude	Longitude	Spatial resolution	No. of pixels
NW	15.75–23.25 N	67.00–73.25 E	0.25° × 0.25°	262
SW	7.75–15.75 N	73.00–77.00 E	0.25° × 0.25°	103
SE	7.25–18.75 N	77.00–85.00 E	0.25° × 0.25°	97
NE	18.75–21.75 N	84.75–89.00 E	0.25° × 0.25°	64

NW, Northwest; SW, Southwest; SE, Southeast; NE, Northeast.

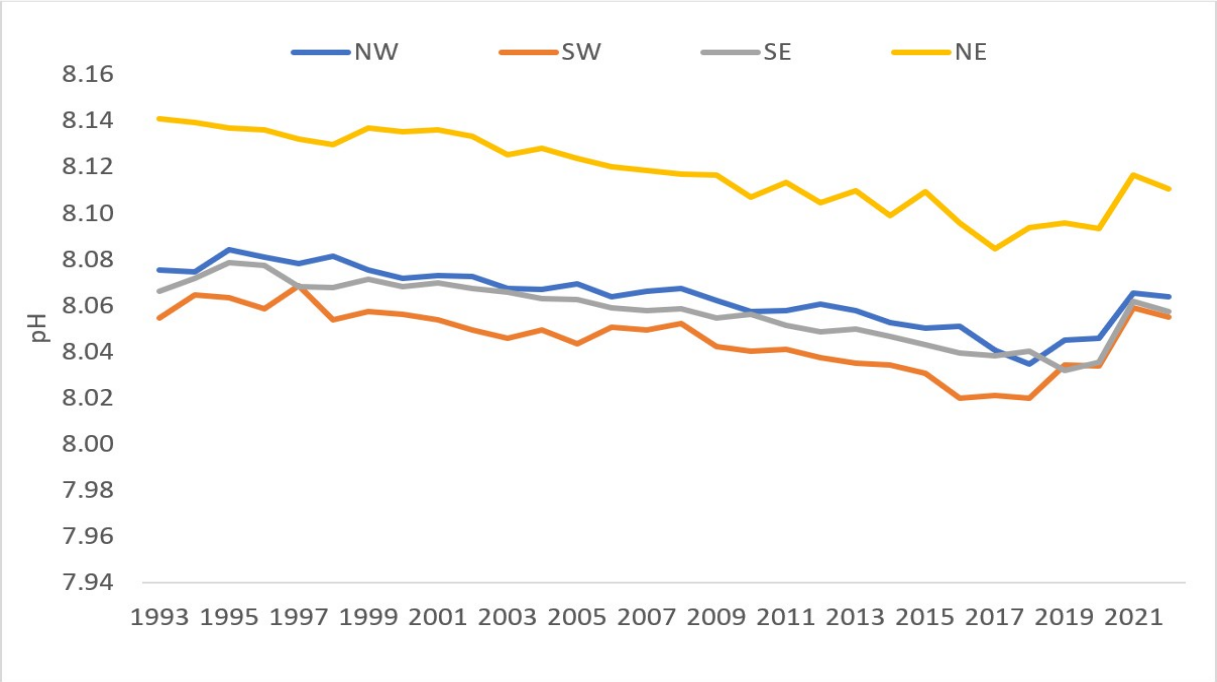

Figure 2. Interannual variations in pH along the four coasts of India.

Table 2. Coast-wise seasonal average pH (mean ± standard deviation) variations from 1993 to 2022

Coasts/Seasons	Monsoon	Post-monsoon	Winter	Summer
NW	8.053 ± 0.017	8.059 ± 0.010	8.085 ± 0.022	8.062 ± 0.006
SW	8.047 ± 0.015	8.021 ± 0.013	8.061 ± 0.008	8.046 ± 0.003
SE	8.029 ± 0.013	8.070 ± 0.030	8.100 ± 0.018	8.046 ± 0.008
NE	8.095 ± 0.038	8.191 ± 0.055	8.157 ± 0.027	8.060 ± 0.006

variations; the post-monsoon season recorded the highest pH (8.191 ± 0.055), reflecting increased alkalinity. Winter showed stable pH levels (8.157 ± 0.027), and summer exhibited the lowest pH variability (8.060 ± 0.006). ANOVA confirmed a highly significant seasonal effect on pH ($F(3, 356) = 231.8$, $p < 0.0001$), with Tukey tests revealing significant differences across all seasonal comparisons ($p < 0.0001$) (Table 3). Spatially, pH levels were higher in the northern coastal regions, particularly during winter and summer, with some areas exceeding 8.20. The southern parts of the northeast coast consistently exhibited slightly lower pH values (Figure 3 *d*).

Principal component analysis

The PCA results indicate that the first principal component (Dimension (Dim) 1) explains 65.75% of the total variance, capturing the majority of the variability in the dataset. The second principal component (Dim. 2) accounts for an additional 19.94%, increasing the cumulative variance to 85.69% (Figure 4). This suggests that the first two dimensions retain most of the information, making them effective for dimensionality reduction and visualisation. The rapid decline in eigenvalues across dimensions highlights that the dataset's structure is largely captured by the first

Table 3. Tukey multiple comparisons of means at 95% family-wise confidence level

Seasons	p-value			
	NW	SW	SE	NE
PM-M	0.075	< 0.001	< 0.001	< 0.001
S-M	0.018	0.782	< 0.001	< 0.001
W-M	< 0.001	< 0.001	< 0.001	< 0.001
S-PM	0.998	< 0.001	< 0.001	< 0.001
W-PM	< 0.001	< 0.001	< 0.001	< 0.001
W-S	< 0.001	< 0.001	< 0.001	< 0.001

p-values obtained from Tukey's HSD multiple comparison test. Comparisons with $p < 0.05$ are considered statistically significant.

Table 4. Principal component analysis (PCA) results

PC's	Eigenvalue	Variance percentage	Cumulative variance percentage
PC1	2.629	65.748	65.748
PC2	0.797	19.943	85.692
PC3	0.511	12.787	98.480
PC4	0.060	1.519	100.00

PC, Principal Components.

two components, supporting their use for further analyses such as clustering or classification (Table 4). The variable contribution analysis revealed key variance and relationships among pH variables (pH_M, pH_PM, pH_W, and pH_S) across four dimensions (Figure 5). The PC1 accounts for the largest variance, with high positive loadings from pH_PM (0.578), pH_W (0.516), and pH_M (0.491), indicating these variables share similar patterns of pH variation. The PC2 highlights contrasting contributions, with pH_W (0.505) showing a strong positive loading, while pH_S (-0.736) contributes negatively, suggesting differentiation between these variables along this axis. PC3 is dominated by pH_M (0.739), showing its distinct variance, whereas pH_S (-0.542) contributes negatively, indicating opposing trends. These results highlight distinct grouping patterns and relationships among the seasons, which can be further analysed for clustering or predictive modelling.

Discussion

Inter-annual variations in pH in marine waters are influenced by both natural and human-related factors, including ocean circulation, temperature changes, carbon dioxide levels, and local environmental conditions. Research investigations projected a decline of upper ocean pH by 0.3–0.4 units by the end of the 21st century[5], which could decrease oceanic biological production[6]. Studies indicate that pH levels can change from year to year, reflecting the effects of phenomena such as El Niño and La Niña, as well as seasonal cycles like the monsoon[29]. The overall trend from 1993 to 2022 shows a gradual decline in pH values in the coastal waters of India ($R^2 = 0.727$). Long-term observations demonstrate a general downward trend in pH in many regions, mainly due to increased atmospheric CO_2, contributing to ocean acidification. The coast-wise pH analysis shows the greatest variability along the northeast coast ($R^2 = 0.80$), followed by the southeast ($R^2 = 0.72$), northwest ($R^2 = 0.71$), and southwest ($R^2 = 0.49$). Local hydrographic conditions and point-source pollution further modulate short-term pH fluctuations[13,7].

Despite regional differences, all coastal zones experienced a minimal overall decline, reflecting stable pH levels over the three decades. The large inter-annual surface pH variability in the Arabian Sea was observed from 1990 to 2013, ranging from 7.93 to 8.65 (ref. 30), which supports the current investigations. The Southern Ocean has shown signs of acidification by decreasing mean rates of pH from 0.0011 to 0.0020 yr^{-1} from 1969 to 2003, which led to serious consequences for marine ecosystems shortly thereafter[9,10]. The significant reduction in pH along the northeast and southeast coasts could be attributed to the reduced freshwater discharge, together with the positive Indian Ocean Dipole event that contributed to enhanced acidification (lowered by 0.01 units) and pCO_2 levels in the coastal western BoB[14].

Along the NW coast, surface pH is generally uniform (7.86–8.06) but punctuated by local highs and lows driven by biological activity, coastal circulation, and urban runoff[31]. The satellite-derived pH values agree with

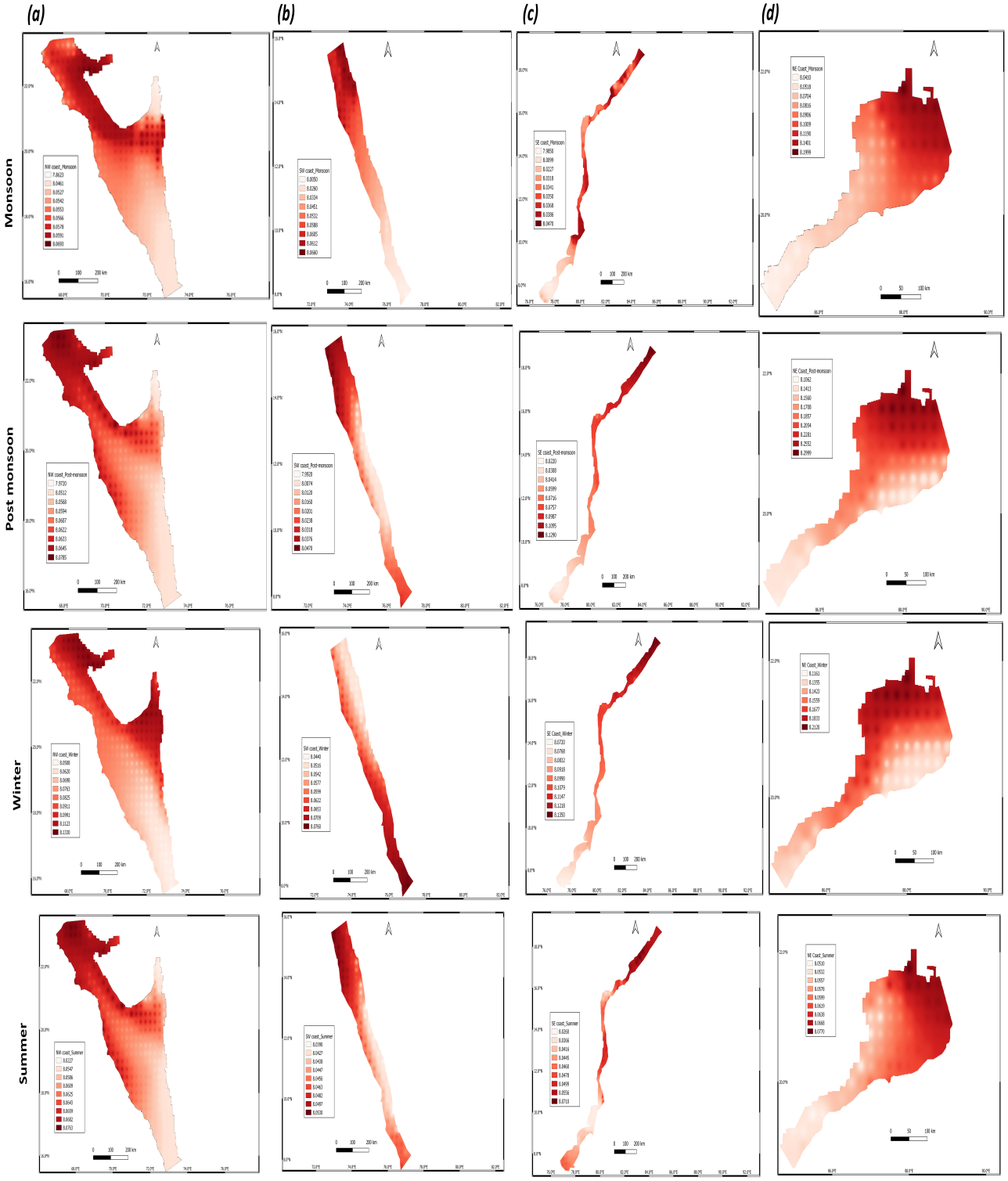

Figure 3. Spatial and temporal variations in pH values along the four coasts (***a***) NW, (***b***) SW, (***c***) SE, and (***d***) NE and four seasons.

earlier reports from the northern Arabian Sea (7.90–8.20) (ref. 32) and the central Arabian Gulf (8.01–8.21) (ref. 12). Seasonally, pH peaks in winter (8.08 ± 0.02) and dips during the monsoon (8.05 ± 0.01), mirroring the winter-

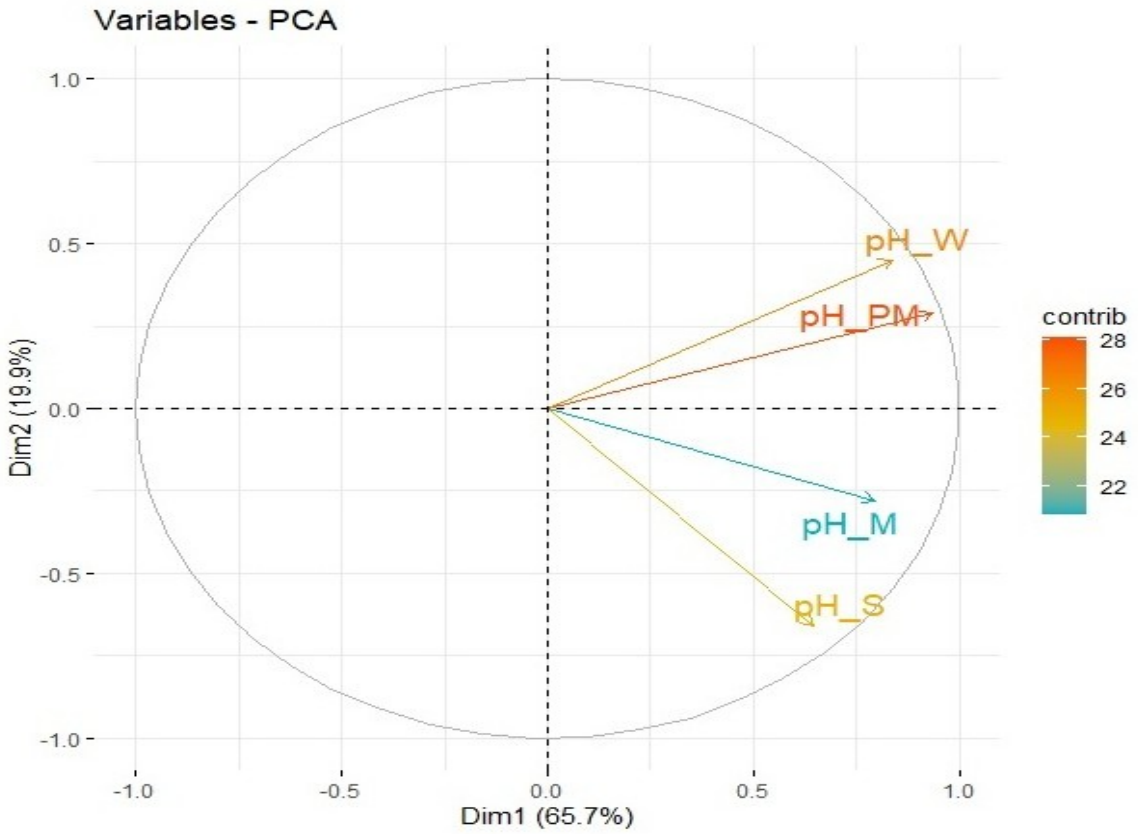

Figure 4. Principal component analysis (PCA) of seasonal pH variability along Indian coasts.

high/summer-low pattern documented for the southeastern Arabian Gulf[33]. SW coastal waters display a narrower pH range during the present study (8.03 – 8.06; mean 8.05 ± 0.01). Here, winter again shows the maximum pH (8.06 ± 0.01), with a minimum in the post-monsoon period (8.02 ± 0.01). The offshore, surface pH in the Arabian Sea varied widely from 7.93 to 8.65 between 1990 and 2013 (ref. 31). In Goa's coastal zone, pH spans 7.6 – 8.1; monsoon lows are linked to upwelling rather than freshwater inputs[17]. Globally, low-pH hotspots coincide with upwelling regions in the tropical Pacific and the Arabian and Bering Seas, whereas subpolar and polar waters exhibit higher pH during spring-summer phytoplankton blooms[32]. Collectively, these patterns highlight the tight coupling of hydrodynamic, climatic, and local biogeochemical processes in regulating coastal pH along India's SW coast.

The southeast coast of India exhibited a mean surface pH of 8.06 ± 0.02. Values declined during the monsoon (8.03 ± 0.01), especially in southern sectors, owing to freshwater inputs, then rebounded in the postmonsoon (8.13) and winter (8.14) seasons when dilution waned and photosynthetic uptake of CO_2 intensified[21]. This spatial variability highlights the influence of seasonal changes, freshwater influx, and coastal processes on ocean chemistry along the southeast coast. The average pH ranges from 8.079 to 8.182 (8.119 ± 0.027) along the northeast coast of India, which is the maximum across the four coasts analysed. Peak values occurred in the postmonsoon (8.19 ± 0.06) and winter (8.16 ± 0.03) periods, consistent with earlier measurements in the Rushikulya estuary (7.90 – 8.11) (ref. 19). Summer (8.06 ± 0.01) and monsoon (8.10 ± 0.04) minima reflect enhanced river discharge, lower salinity, and organic-matter decomposition[34]. Across all coasts, near-shore waters consistently displayed higher pH than adjacent offshore zones, underscoring the influence of coastal photosynthesis, freshwater fluxes, and anthropogenic inputs on carbonate equilibria[4].

The PCA results illustrate pH variations along the NW, SW, SE, and NE coasts of India. The first two principal components (Dim.1 and Dim.2) explain 65.7% and 19.9% of the total variance, respectively (Figure 6). The plot shows clear regional clustering, with the NE coast (blue) exhibiting the largest variability and the NW coast (yellow) forming a tightly clustered group, suggesting more consistent pH patterns. The SE (red) and SW (cyan) coasts show some overlap but remain distinguishable, indicating shared yet regionally specific influences on pH variability. The

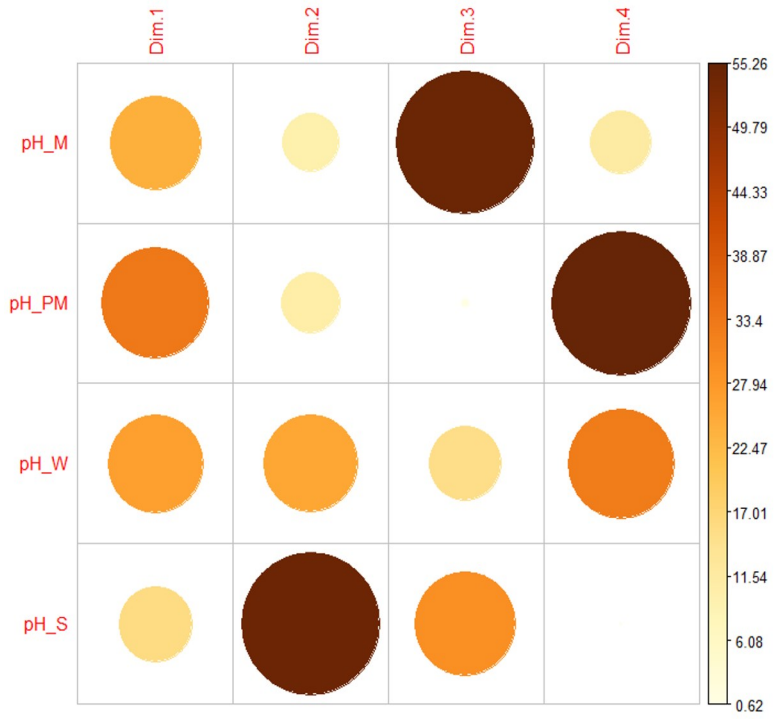

Figure 5. Correlation matrix of pH parameters for principal component contributions.

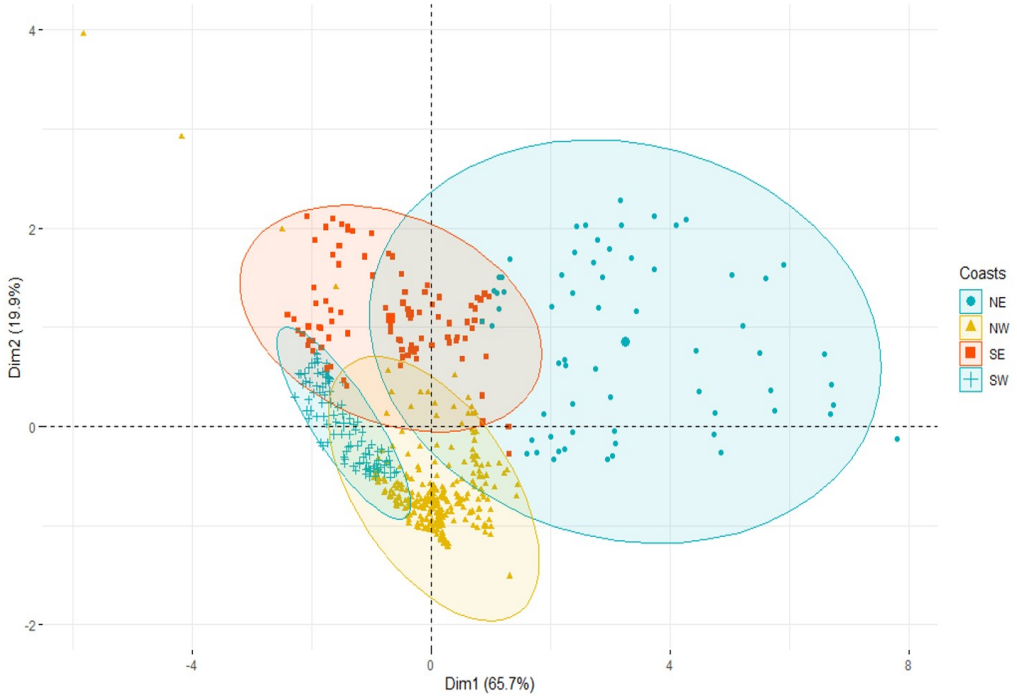

Figure 6. PCA of coastal regions (NW, SW, SE, and NE): visualisation of grouped individuals across dimensionality reduction axes.

confidence ellipses further highlight the distinct seasonal pH dynamics across these coastal regions. For example, the NE and SW coasts, characterised by higher variability, may require targeted monitoring and interventions to address

the impacts of freshwater inputs and eutrophication. In contrast, with relatively stable pH, the SE and NW coasts provide opportunities to investigate long-term trends and resilience to climate change.

The multivariate analysis provides valuable insights into the seasonal pH variability and the underlying factors influencing these patterns. Dim.1 (46% of total variance) carries strong positive loadings for post-monsoon (0.58), winter (0.52), and monsoon pH (0.49), underscoring their common dependence on river discharge and nutrient regeneration[33]. Dim.2 (28%) separates winter (+0.51) from summer (–0.74) conditions, reflecting the well-known contrast between CO_2 drawdown during cool, high-productivity months and dilution–stratification effects in summer[32,35]. Dim.3 (15%) is dominated by monsoon pH (+0.74) against a negative summer influence (–0.54), indicating that freshwater-driven acidification during peak discharge is largely decoupled from summer dynamics[36]. Together, these axes reveal that riverine fluxes, biological CO_2 uptake, and seasonal stratification jointly regulate the observed pH variability in the region.

Summary

The satellite-derived pH offers a detailed understanding of pH variability across time and space in India's coastal waters, providing a basis for clustering and predictive modelling. It delivers comprehensive pH variability data over longer periods and broader areas. Higher average pH levels were observed in the NE coastal waters, followed by the NW, SE, and SW coasts. The strong influence of monsoonal processes on pH emphasises the need for integrated management strategies that account for seasonal fluctuations and freshwater inputs. Significant temporal variability was noted, with higher pH levels during winter on the NW, SW, and SE coasts. The difference between summer and winter pH highlights the roles of biological activity and temperature in seasonal carbonate chemistry. This study is a pioneering effort in the region, revealing pH variability over three decades and across four coasts. Overall, the multivariate analysis effectively identifies seasonal and regional patterns in pH variability and underlines the importance of seasonal hydrodynamics, biological processes, and regional freshwater influence in shaping pH distribution, offering a framework for further analysis through clustering or predictive models. The distinct clustering patterns demonstrate the need for localised studies to develop accurate predictive models and promote sustainable coastal management. Additionally, the present study provides an early warning system for climate-change-induced ocean acidification, supporting timely interventions to protect biodiversity and enhance carbon cycle resilience.

Conflict of interest: The authors declare that there is no conflict of interest.

Funding: No funding was received to execute the present study.

Data availability statement: The datasets generated and analysed during the present study are available from the corresponding author on reasonable request.

1. Gattuso, J. P., Bijma, J., Gehlen, M., Riebesell, U. and Turley, C., Ocean acidification: knowns, unknowns, and perspectives. In *Ocean Acidification* (eds Gattuso, J. P. and Hansson, L.), Oxford University Press, Oxford, UK, 2011, pp. 291–311.
2. Chakraborty, K., Valsala, V., Bhattacharya, T. and Ghosh, J., Seasonal cycle of surface ocean pCO_2 and pH in the northern Indian Ocean and their controlling factors. *Prog. Oceanogr.*, 2021, **198**; https://doi.org/10.1016/j.pocean.2021.102683.
3. Feely, R. A., Doney, S. C. and Cooley, S. R., Ocean acidification: Present conditions and future changes in a high-CO_2 world. *Oceanography*, 2009, **22**(4), 36–47; https://doi.org/10.5670/oceanog.2009.95.
4. Cai, W. J. *et al.*, Acidification of subsurface coastal waters enhanced by eutrophication. *Nat. Geosci.*, 2011, **4**(11), 766–770; https://doi.org/10.1038/ngeo1297.
5. Kwiatkowski, L. and Orr, J. C., Diverging seasonal extremes for ocean acidification during the twenty-first century. *Nat. Clim. Change*, 2018, **8**(2), 141–145; https://doi.org/10.1038/s41558-017-0054-0.
6. Raper, S. C., Giorgi, F., Lovejoy, T. E. and Hannah, L., Climate change projections and models. In *Climate Change and Biodiversity* (eds Lovejoy, T. E. and Hannah, L.), Yale University Press, New Haven, CT, USA, 2005, pp. 199–210.
7. Caldeira, K. and Wickett, M. E., Anthropogenic carbon and ocean pH. *Nature*, 2003, **425**(6956), 365; https://doi.org/10.1038/425365a.
8. Orr, J. C. *et al.*, Anthropogenic ocean acidification over the twenty-first century and its impact on calcifying organisms. *Nature*, 2005, **437**(7059), 681–686; https://doi.org/10.1038/nature04095.
9. Hauck, J., Hoppema, M., Bellerby, R. G. J., Völker, C. and Wolf-Gladrow, D., Data-based estimation of anthropogenic carbon and acidification in the Weddell Sea on a decadal timescale. *J. Geophys. Res. Oceans*, 2010, **115**(C3); https://doi.org/10.1029/2009JC005479.
10. Midorikawa, T., Inoue, H. Y., Ishii, M., Sasano, D., Kosugi, N., Hashida, G. and Suzuki, T., Decreasing pH trend estimated from 35-year time series of carbonate parameters in the Pacific sector of the Southern Ocean in summer. *Deep-Sea Res. I: Oceanogr. Res. Pap.*, 2012, **61**, 131–139; https://doi.org/10.1016/j.dsr.2011.12.003.
11. Al-Mutairi, M. *et al.*, Temporal variations in abundance and species richness of phytoplankton with emphasis on diatoms in the subtidal waters of Umm Al-Namil Island, north-western Arabian Gulf of the ROPME Sea Area. *J. Environ. Biol.*, 2020, **41**(6), 1470–1485; https://doi.org/10.22438/jeb/41/6/MRN-1151.
12. Elobaid, E. A., Al-Ansari, E. M., Yigiterhan, O., Aboobacker, V. M. and Vethamony, P., Spatial variability of summer hydrography in the central Arabian Gulf. *Oceanologia*, 2022, **64**(1), 75–87; https://doi.org/10.1016/j.oceano.2021.09.003.
13. Zeebe, R. E. and Wolf-Gladrow, D., *CO_2 in Seawater: Equilibrium, Kinetics, Isotopes*, Elsevier Science, Amsterdam, Netherlands, 2001, vol. 65. p. 24.
14. Sarma, V. V. S. S., Paul, Y. S., Vani, D. G. and Murty, V. S. N., Impact of river discharge on the coastal water pH and pCO_2 levels during the Indian Ocean Dipole (IOD) years in the western Bay of Bengal. *Cont. Shelf Res.*, 2015, **107**, 132–140; https://doi.org/10.1016/j.csr.2015.07.013.

15. Bhadja, P. and Kundu, R., Status of the seawater quality at few industrially important coasts of Gujarat (India) off Arabian Sea. *Indian J. Geo-Mar. Sci.*, 2012, **41**(1), 90–97.
16. Vase, V. K. *et al.*, Spatio-temporal variability of physico-chemical variables, chlorophyll a, and primary productivity in the northern Arabian Sea along India coast. *Environ. Monit. Assess.*, 2018, **190**(3); https://doi.org/10.1007/s10661-018-6490-0.
17. Shetye, S. S., Naik, H., Kurian, S., Shenoy, D., Kuniyil, N., Fernandes, M. and Hussain, A., pH variability off Goa (eastern Arabian Sea) and the response of sea urchin to ocean acidification scenarios. *Mar. Ecol.*, 2020, **41**(5); https://doi.org/10.1111/maec.12614.
18. Soman, C., Lal, D. M., Haridas, H., Deshmukhe, G., Jaiswar, A. K., Shenoy, L. and Nayak, B. B., Spatial and temporal dynamics of water quality along coastal waters of Mumbai, India. *Arab. J. Geosci.*, 2022, **15**(2); https://doi.org/10.1007/s12517-021-09374-4.
19. Baliarsingh, S. K., Srichandan, S., Naik, S., Sahu, K. C., Lotliker, A. A. and Kumar, T. S., Distribution of hydro-biological parameters in coastal waters off Rushikulya Estuary, East Coast of India: A pre-monsoon case study. *Pak. J. Biol. Sci.*, 2013, **16**(16), 779–787; https://doi.org/10.3923/pjbs.2013.779.787.
20. Sarma, V. V. S. S., Krishna, M. S., Paul, Y. S. and Murty, V. S. N., Observed changes in ocean acidity and carbon dioxide exchange in the coastal Bay of Bengal: A link to air pollution. *Tellus B: Chem. Phys. Meteorol.*, 2015, **67**(1); https://doi.org/10.3402/tellusb.v67.24638.
21. Vajravelu, M., Martin, Y., Ayyappan, S. and Mayakrishnan, M., Seasonal influence of physico-chemical parameters on phytoplankton diversity, community structure and abundance at Parangipettai coastal waters, Bay of Bengal, South East Coast of India. *Oceanologia*, 2018, **60**(2), 114–127; https://doi.org/10.1016/j.oceano.2017.10.003.
22. Sarangi, R. K. and Behera, S., Coastal water quality assessment using satellite remote sensing techniques: case studies along the Indian coastline. *Mar. Pollut. Bull.*, 2020, **150**; https://doi.org/10.1016/j.marpolbul.2019.110701.
23. European Union-Copernicus Marine Service, Global Ocean Biogeochemistry Hindcast. Mercator Ocean International, 2018; https://doi.org/10.48670/moi-00019. (accessed on 3 October 2024).
24. European Union-Copernicus Marine Service, Global Ocean Biogeochemistry Analysis and Forecast. Mercator Ocean International, 2019; https://doi.org/10.48670/moi-00015. (accessed on 5 February 2025).
25. European Union-Copernicus Marine Service, Global Ocean Physics Reanalysis. Mercator Ocean International, 2018; https://doi.org/10.48670/moi-00021. (accessed on 24 April 2025).
26. Bittig, H. C. *et al.*, An alternative to static climatologies: robust estimation of open ocean CO_2 variables and nutrient concentrations from T, S, and O_2 data using Bayesian neural networks. *Front. Mar. Sci.*, 2018, **5**; https://doi.org/10.3389/fmars.2018.00328.
27. Feldman, G. C., SeaDAS SeaWiFS Data Analysis System, NASA Goddard Space Flight Center, 2021; https://seadas.gsfc.nasa.gov/history/.
28. QGIS Development Team, QGIS Geographic Information System, Open Source Geospatial Foundation Project, 2023; https://qgis.org.
29. Isa, N. S., Akhir, M. F., Kok, P. H., Daud, N. R., Khalil, I. and Roseli, N. H., Spatial and temporal variability of sea surface temperature during El-Niño Southern Oscillation and Indian Ocean Dipole in the Strait of Malacca and Andaman Sea. *Reg. Stud. Mar. Sci.*, 2020, **39**; https://doi.org/10.1016/j.rsma.2020.101402.
30. Tarique, M., Rahaman, W., Fousiya, A. A., Lathika, N., Thamban, M., Achyuthan, H. and Misra, S., Surface pH record (1990–2013) of the Arabian Sea from boron isotopes of Lakshadweep corals: trend, variability, and control. *J. Geophys. Res. Biogeosci.*, 2021, **126**(7); https://doi.org/10.1029/2020JG006122.
31. Zingde, M. D., Sharma, P. and Sabnis, M. M., Physico-chemical investigations in Auranga River Estuary (Gujarat). *Mahasagar*, 1985, **18**(1), 31–38.
32. Reichart, G.-J., Lourens, L. J. and Zachariasse, W. J., Temporal variability in the northern Arabian Sea oxygen minimum zone (OMZ) during the last 225,000 years. *Paleoceanography*, 1998, **13**(6), 607–621; https://doi.org/10.1029/98PA02203.
33. Mezhoud, N., Temimi, M., Zhao, J., Al Shehhi, M. R. and Ghedira, H., Analysis of the spatio-temporal variability of seawater quality in the southeastern Arabian Gulf. *Mar. Pollut. Bull.*, 2016, **106**(1–2), 127–138; https://doi.org/10.1016/j.marpolbul.2016.03.016.
34. Rajasegar, M., Srinivasan, M. and Khan, S. A., Distribution of sediment nutrients of Vellar Estuary in relation to shrimp farming. *Indian J. Mar. Sci.*, 2002, **31**(2), 153–156.
35. Ravichandran, C., Moses, A. A., Girija, K. and Chakravarthy, P. P. S., Drinking water quality assessment in few selected pilgrim centres and tourist spots in Tamil Nadu. *Indian J. Environ. Prot.*, 2002, **22**(2), 129–136.
36. Naqvi, S. W. A., Naik, H., Pratihary, A., D'Souza, W., Narvekar, P. V., Jayakumar, D. A. and Saino, T., Coastal versus open-ocean denitrification in the Arabian Sea. *Biogeosciences*, 2006, **3**(4), 621–633; https://doi.org/10.5194/bg-3-621-2006.

ACKNOWLEDGEMENTS. The authors thank the Indian Council of Agricultural Research (ICAR), Kochi; the Director, ICAR-Central Marine Fisheries Research Institute (CMFRI), Kochi; the Scientist In-Charge, Veraval Regional Station; and the Head, Fishery Resources Assessment, Economics and Extension Division, ICAR-CMFRI, Kochi, for the encouragement and support during the present study. The research work was done under the National Innovations in Climate Resilient Agriculture project.

Received 10 December 2025; accepted 22 May 2026.

doi: 10.18520/cs/v130/i12/1077-1086